J Nanostruct 15(4): 1733-1744, Autumn 2025

RESEARCH PAPER

Synthesis, Characterization of New Nanocomplex and Lifetime Study of Polyvinyl Chloride and Polystyrene Polymers

A. Ali [1], B. E. Jasim [2], N. A.A. Aboud [2], Kamal Rashid Al-Jorani [1], A. S. Al-Sammak [3], Ahmed A. Ahmed [4]*

[1] *Department of Chemistry, College of Science, University of Wasit, Kut, 52002, Iraq*

[2] *Department of Chemical Industrial, Institute of Technology, Middle Technical University, Al Zafaraniya,10074, Baghdad, Iraq*

[3] *Polymer Research Unit, College of Science, Al- Mustansiriyah University, Al- Mustansiriyah, 10052, Baghdad, Iraq*

[4] *Department of Chemistry, College of Engineering, University of Wasit, Wasit, 52001, Iraq*

ARTICLE INFO

Article History:
Received 09 June 2025
Accepted 27 August 2025
Published 01 October 2025

Keywords:
1, 2, 4-Triazole
Nanocomplex
Polystyrene
Polyvinyl Chloride
Sonochemical

ABSTRACT

The ligand 5-(naphthalen-1-ylmethyl)-4-(((1E,2E)-3-phenylallylidene) amino)-4H-1,2,4-triazole-3-thiol in micro size used to synthesize the new cobalt nanocomplex using the sonochemical method. The new cobalt nanocomplex[Dichlorobis(5-(naphthalen-1-ylmethyl)-4-(((1E,2E)-3-phenylallylidene) amino)-4H-1, 2, 4-triazole-3-thiol) cobalt(II)] hydrate, was diagnosed by spectroscopic methods X-Ray diffraction, where the average crystal of the prepared particles was (45 nm), and using the Field Emission Scanning Electron Microscopy (FESEM) the average nano size was about (41 nm) and Atomic force microscopy (AFM) statistical distribution of diameters showed results within the nanomaterial limit (62.72 nm) this is consistent with the measurements of both (X-Ray Diffraction) and (FESEM). Also, pure polyvinyl chloride (PVC) and polystyrene (PS) films were prepared alone, and in the presence of the inorganic nano complex prepared as an additive; the follow-up of the optical fragmentation and photoinhibition of the polymeric films prepared with the presence and absence of the nano complex, the accelerated irradiation device, which had an intensity of 4×10^{-5} einstine.ed^{-3}.sec and by using the infrared absorbance (FTIR). Hydroxyl groups (I_{OH}), carbon (I_{CO}), and polyene (I_{PO}) for polyvinyl chloride and polystyrene with and without the addition of cobalt nanocomplex with the irradiation time, as well as the ultraviolet radiation absorption to calculate the photodissociation speed constant of the polymeric films, in addition to the weight loss and changes on the surface of the films. The impact of temperature, and light, on the lifetime of Polyvinyl chloride and Polystyrene Polymers has been studied in the presence and absence of the nanocomplex. In general, increased stability and lifetime of polymers were observed in the presence of the nanocomplex.

How to cite this article
Ali A., Jasim B., Aboud N., Al-Jorani K., Al-Sammak A., Ahmed A. Synthesis, Characterization of New Nanocomplex and Lifetime Study of Polyvinyl Chloride and Polystyrene Polymers. J Nanostruct, 2025; 15(4):1733-1744. DOI: 10.22052/JNS.2025.04.022

* *Corresponding Author Email: kaljorani@uowasit.edu.iq*

INTRODUCTION

Due to their simplicity of synthesis, excellent complexation capabilities with a variety of transition metals, and amazing biological activity, particularly in their complexes, Schiff base ligands have drawn the attention of numerous researchers [1]. The contain both soft and hard donor atoms and have high sensitivity and selectivity in coordination as well as extensive reaction properties, Schiff base, which include S, N, and O atoms as electron-donating groups, form stable chelates with a wide range of metals and can be extremely useful as antibacterial, antifungal, antitumor, antioxidant, anticancer, antiviral, antimalarial, anti-inflammatory, anti-HIV, antiparasitic agents [2, 3] and anti-cancer [4].

1,2,4-triazole, various biological activities can be derived from Schiff base compounds, which have an azomethine group in their structure. The capacity of Schiff-triazole base ligands to regulate the steric and electrical characteristics of the bonds affixed to metal ions is their primary benefit [5-7].

The chemicals' physicochemical, pharmacological, toxicological, and pharmacokinetic qualities are thereby improved by their lipophilicity and polarity. Strong coordination capacity with metal ions is provided by all three of the triazole's nitrogen atoms [8, 9]. Because 1,2,4-triazole-derived chelate base compounds feature extra N-donor atoms (N-donor) that can form single, double, or triple bonding sites and boost stability through the alkylating action, they have drawn a lot of attention recently [10]. Furthermore, because of their varied coordination patterns, ligands derived from triazole have been used to create a variety of complexes with amazing properties by sharing metal ions' positive charge with the N-donor atoms of 1,2,4-triazole. This has increased the stability of the chelate ring by delocalizing the π-electron cloud.

1,2,4-triazole-derived compounds have drawn a lot of interest recently because of the main issues related to the application of whether synthetic or semi-synthetic; one of the main issues with using polymeric materials is that they photodegrade under severe conditions like sunshine and high temperatures [11, 12]. Discoloration, cross-linking, and chain cleavage may result from this [13], To avoid and/or reduce the impact of atmospheric conditions, polymeric materials must be stabilized against photodegradation and photooxidation. Stabilization would also expand the polymer's long-term applications, boosting its economic feasibility. Polymeric films can be made more photostable by adding different additives, such as plasticizers [14] and heterocyclics [15].

Polymers are widely used due to their many beneficial characteristics; if the decomposition, disintegration, fragmentation, durability, or resistance of materials determine their utility, additives, chemical combinations, and other substances can quicken the pace of fragmentation or affect the stabilization and hardening of materials. Comparing blended and unblended PVC-based plastics [16-18].

These polymers are the most prevalent kind of plastic, accounting for 90.3% (plus the remaining 9.7%) of all polymeric materials used [19]. Furniture, cars, houses, structures, emergency shelters, medications, cold storage, chemical manufacture, and food packaging are all made of polymers [20, 21].

Synthetic aromatic polymer, or polystyrene (PS), is manufactured annually in millions of tons. The plastic that is created by polymerizing styrene finds widespread application. Polystyrene comes in a variety of forms and applications, including insulation, electronics [22], bottles, and containers. Its characteristics are determined mainly by where the phenyl groups are located in the polymer chain [23, 24].

The photochemical process (degradation) of exposed polymers and plastics is stopped or slowed down by the photoinhibition of polymers. By adding a mild stabilizer to the polymer, the rate of oxidation is slowed down [25, 26]. One example of a method used to avoid or prevent the effect of ultraviolet radiation on plastics is azo dyes, which are complex formulas that are insoluble in inorganic, organic, and metallic compounds, such as anthraquinone dyes, and are perfect UV reflectors. This polymer has been the focus of extensive research because of its impact on the physical, chemical, and mechanical properties of PVC and PS, which react significantly to light and heat (typically because of the loss of hydrochloric acid). The creation of polyvinyl chloride requires the usage of vinyl chloride monomer, one of the most precious goods in the chemical sector [27]. An investigation has been conducted into how adding nanoparticles to a polymer can help with the photostabilization process 10 times the angstrom, the fundamental unit of atomic

size, is researched as the "basic principles of molecules and compounds". Nanomaterial research and its applications in various scientific fields are the main areas of interest in the field of nanotechnology [28]. To be more precise, their distinctive characteristics stem from their higher surface area-to-volume ratio [29-33].

MATERIALS AND METHODS

All chemicals were obtained from Sigma-Aldrich and were analytical-grade reagents that did not require additional purification. Diagnostic tools were used to prepare and identify the nano complex; the sonochemical reactions were carried out by the sonochemical probe (Ultrasonic Processor UP200S, Hielscher Ultrasound Technology, U.K.), atomic force microscope images of the surface compounds are measured by using (SPM model AA 300 of Angstrom Advanced INC USA), and the nanoparticle complexes' size and morphology were characterized using a field emission scanning electron microscope ((FE-SEM) TESCAN, MIRA3, France). At the same time, X-ray diffraction is the primary technique used to identify the crystalline solid structure. X-ray diffraction experimentations characterized by using (Xpert, Phillips, Holland).

Preparation of (5-(naphthalen-1-ylmethyl)-4-(((1E,2E)-3-phenylallylidene) amino)-4H-1,2,4-triazole-3-thiol) ligand (L)

Through the method described in the reference [3], ligand (5-(naphthalen-1-ylmethyl)-4-(((1E,2E)-3-phenylallylidene)amino)-4H-1,2,4-triazole-3-thiol) was obtained and confirmed by the diagnostic methods (S2-S7) mentioned in the Supplementary Materials file.

Synthesis of nano complex ([Dichlorobis(5-(naphthalen-1-ylmethyl)-4-(((1E,2E)-3-phenylallylidene)amino)-4H-1,2,4-triazole-3-thiol) cobalt(II)] hydrate) (CoL)

Using sonochemical synthesis (an ultrasonic device), the new nanocomplex CoL was synthesized using a micro-sized ligand. As a result, the 1,2,4-triazole Schiff base ligand L (0.002 mol, 0.72 g) was dissolved in 30 mL of methanol solvent. Additionally, (0.001 mol, 0.23 g) of the metal salt ($CoCl_2.6H_2O$) was dissolved in 20 mL of methanol, and the metal to ligand (M:L) ratio was 1:2 to synthesize the CoL cobalt nano complex. Finally, the metal solution was added (dropwise) to the ligand solution above. The mixture was exposed to ultrasound radiation for an hour, but intermittently, using a high-intensity ultrasound probe. After the complex precipitated, it was filtered and dried at 50 °C.

Synthesis of Modified Polymeric Films

The 100 milliliters of Tetrahydrofuran (THF) were mixed with five grams of PVC and PS to create the polymer. Following total dissolving, 0.01 g of the nanocomplex was added and continuously stirred for an hour. The mixture was then poured into dimensions (5*5) cm glass molds with a 40 µm thickness.

Polymer films were prepared by dissolving one gram of the polymer in the appropriate solvent. Styrene polymer was dissolved in chloroform, while polyvinyl chloride was dissolved in tetrahydrofuran. They were then placed in locally made glass molds and left at room temperature for 24 hours. After that, the films were removed from the glass molds, the thickness was measured using a 2610A micrometer, and they were glued to cardboard sheets.

Polymeric films with the complex were prepared by adding 0.01 g of the complex to the prepared solution in a round-bottomed flask and refluxing for an hour, then pouring into locally made glass molds and leaving for 24 hours, then placing them on a carton and irradiating them [39].

Photodegradation measuring methods

The films undergo treatment utilizing an accelerated weather meter called QUV (Q-panel Laboratory Ultraviolet testing), which exposes them to ultraviolet (UV) radiation at a temperature significantly higher than 250–380 nm.

Films are tested in the QUV by subjecting them to controlled high temperatures and alternating cycles of UV light and humidity. Using fluorescent UV lights, the QUV replicates the effects of sunlight and uses condensed moisture and/or water spray to replicate dew and rain. Based on earlier research, 300 hours of testing with artificial UV lamps is comparable to almost a year of sunlight, heat, and humidity in Iraq. Thus, the created polymer films are subjected to ambient conditions for a whole year [40, 41].

Weight loss method

The losing weight ratios of photodegraded PVC film in the presence and absence of additives are

used to calculate the stabilizing strength of an addition using the following Eq. 1 [18]:

$$\text{Weight loss } \% = \frac{W_1 - W_2}{W_1} * 100 \quad (1)$$

Where: W_1= weight of sample (before irradiation), W_2= weight of sample (after irradiation).

FTIR Spectra

Using FTIR spectra in the 4000-400 cm^{-1} range, the degree of photodegradation of the polymer films was ascertained utilizing Eq. 2 [15].

$$Is = As / Ar \quad (2)$$

Where: Is = Index of the group under study, As = Absorbance of peak under study, Ar = Absorbance of reference peak.

The ratio of transmittance (%T) to absorptivity (A) is changed using the Beer-Lambert law as in Eq. 3 [35].

$$A = \log \log (100 \backslash T\ \%) \quad (3)$$

RESULTS AND DISCUSSION

Characterization of cobalt nano complex (CoL)

The ligand spectrum showed the vibration spectrum of the υ C=N group for the Schiff base at 1643 cm^{-1}. As for the nano complex (CoL) appearing in Figs. (S2 and S8), its frequency distance in these groups is at 1629 cm^{-1}. This is evidence of the formation of the complex. As for the υ C=S triazole group's bands in the ligand were 1330 cm^{-1} and appeared in the nano complex at 1311 cm^{-1}. This is evidence of the formation of the complex. The association of the metal ion with the sulfur atom with a coordination bond (Co-S) in the thione group [34], aromatic υ (C=N) triazole, and (N-H) groups showed bands at 1595 and 3211 cm^{-1} in FTIR spectrum for ligand respectively, while the characteristic bands at 1602 and 3269 cm^{-1} respectively in nano complex.

The difference in the position and intensity of the C=N azomethine group between the ligand and complex in the FTIR spectra gives more evidence for coordinating the metal ion with C=N nitrogen. As a result of the metal ion being coordinated with the thion sulfur and azomethine nitrogen when complexing, a stable five-membered ring is formed. Also, the difference in new vibration bands for the complex appeared not present in the ligand spectrum of the (Co-S and Co-N) groups at 524 and 459 cm^{-1}, respectively [35].

X-ray diffraction (XRD)

The main technique used in the identification of the crystalline solid structure. X-ray diffraction experimentations are characterized by using (Xpert, Phillips, and Holland), which is characterized by being a continuous scanning device with a speed of 5 deg./min., to identify the noncomplex and determine their crystalline shape using the X-ray diffraction technique. The X-ray tube produces

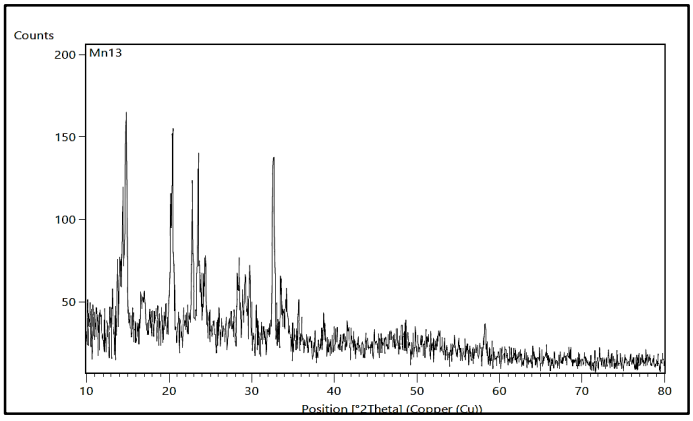

Fig. 1. Shows the X-ray diffraction spectrum of the cobalt nanocomplex.

X-rays using a copper target and a current of 30 mA and voltage of 40 KV., with rays produced is 1.45 A˚. The X-ray diffraction measurement results in (Fig. 1) clearly show an increase in the full width of the middle of the height (FWHM). This indicates the formation of an inorganic nanoparticle complex with an average crystal size of 45 nm. The Debye–Sherrer equation [36] was utilized to calculate the size of the crystal Eq. 4.

$$D = \frac{k\lambda}{\beta \cos \theta} \quad (4)$$

Where λ is the wavelength used, β is the width of the highest peak from the middle, and Θ is the diffraction angle.

Field Emission Scanning Electron Microscopy (FE-SEM)

FE-SEM analyses of the nano complex were also conducted using SEM (Scanning Electron Microscope). Fig. 2 image demonstrates that the sample's morphology is generally spherical, with uniform particles and just a small amount of agglomeration [27]. Owing to the crystals' interrelationships, the agglomeration may be caused by agglomeration spaces with varying diameters. The average grain size in the images was measured with a measuring tool, and the results showed that the average grain size from the scanning electron microscope was approximately 41 nm, which is consistent with the sizes obtained using the X-ray

Atomic force microscope (AFM)

Using AFM data and statistical distribution of the diameters, we observed that the complex gave an average diameter within the nanomaterial's limits (62.72 nm), as shown in (Table 1 and Fig. 3), the 3D nanocomplex and distribution chart of the nanocomplex.

Polymer film diagnosis

The weight loss results as a function of irradiation time [37] are represented in Fig. 4. The results

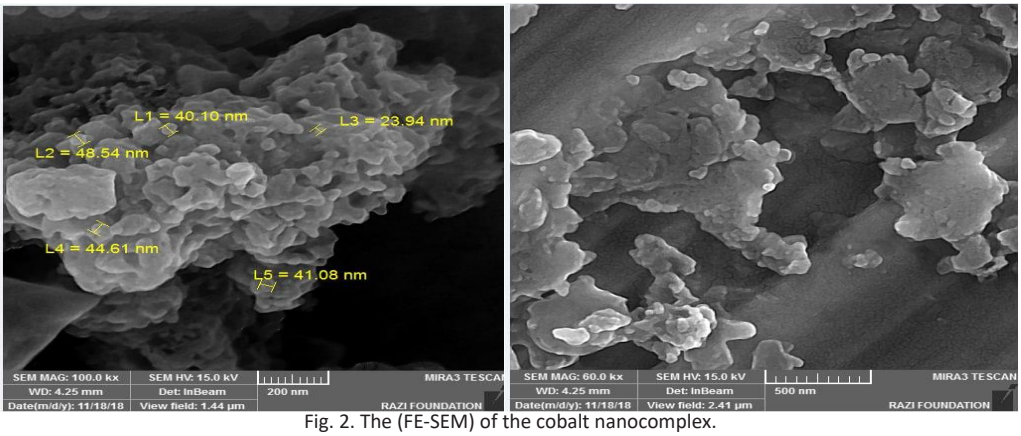

Fig. 2. The (FE-SEM) of the cobalt nanocomplex.

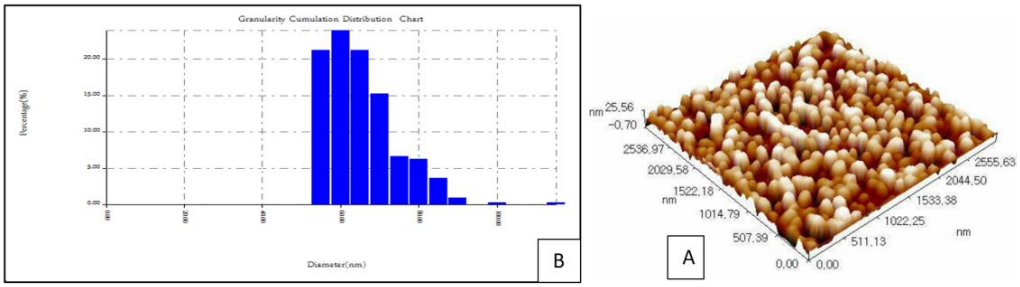

Fig. 3. (A) The 3D nanocomplex, and (B) The distribution chart of the nanocomplex.

indicate that the inorganic nano-complex has an inhibitory effect against the photodegradation of PS and PVC samples, which resulted in a significant decrease in the weight loss percentage compared to the single polymer, and the inhibition efficiency is arranged as follows:

PVC < (PS + nanocomp) < PS< (PVC+ nanocomp.)

AFM and microscopic imaging

Before and after the 300-hour irradiation process, PS and PVC polymer films containing the nanocomplex were subjected to AFM analysis to enhance the clarity of the films' surface topography and provide a precise account of the nanosize distribution ratios and surface roughness. As shown in Fig. 5 and Table 2, the polystyrene with the nano complex after the irradiation procedure had the highest Root mean square (RMS) rate for the films, with a limit of 9.10nm, as is evident in the table of RMS values.

The effect of UV radiation on the surface of PVC and polystyrene with the addition of the nano-inorganic complex was investigated using microscopic images of the polymers. The degree of damage on the surface of the film was shown, where the formation of cracks and holes resulting from the fragmentation and decomposition of the polymer was observed after 300 hours of irradiation in the air. The growth of cracks and grooves with time from UV radiation and the increase in the visual fragmentation of the PVC film, on the other hand, we note that polystyrene films have fewer cracks, which can be inferred as a preference for hot weather conditions. The reason for the formation of tiny cracks and grooves on the surface of the polymer is the result of reactions and shearing of the polymer chains due to radiation exposure, which occurs by breaking the pattern and bonds that produce small parts and fragmentation of the irradiated polymer, which leads to an increase in channels and voids. In the presence of oxygen, it spreads over most of the polymer and causes oxidation.

The addition of the nanomaterial stabilized the polymer and increased its stability, as the stability

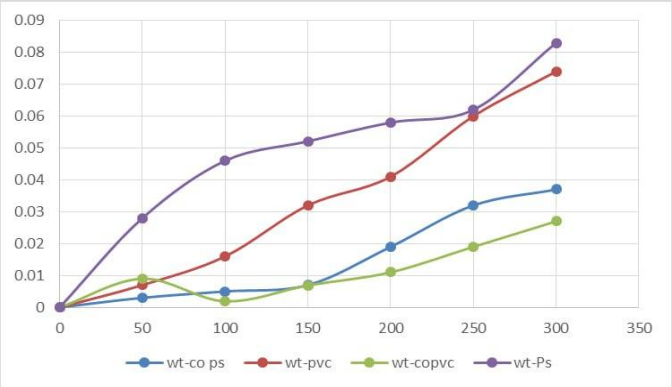

Fig. 4. The weight loss during the irradiation time of the PVC

Table 1. Shows diameter (nm) with percentage for cobalt nano complex.

Diameter (nm)<	Volume (%)	Cumulation (%)
55.00	21.26	21.26
60.00	23.92	45.18
65.00	21.26	66.45
70.00	15.28	81.73
75.00	6.64	88.37
80.00	6.31	94.68
85.00	3.65	98.34
90.00	1.00	99.34
100.00	0.33	99.67
115.00	0.33	100.00

of the polymer exposed to radiation depends on the chemical composition of the material. The incident radiation excites the chemical system, so adding materials containing aromatic rings in their composition absorbs energy, which greatly increases the stability of polymers exposed to radiation by redistributing the excited energy throughout the material, especially if it is a nano complex containing an inorganic metal characterized by a high surface area. Fig. 6 represents microscopic images of polymers impregnated with inorganic nanomaterials. Their

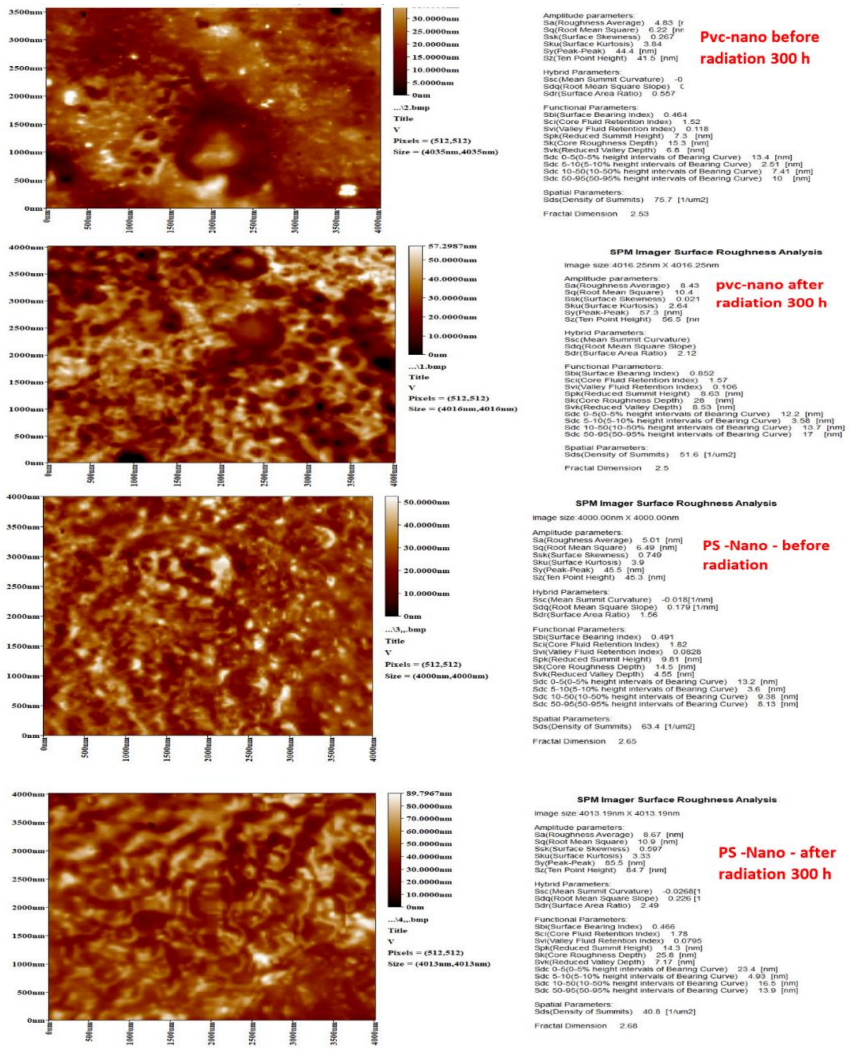

Fig. 5. The AFM measurements and 3D images of the PVC and PS polymer films with the nanocomplex before and after irradiation for 300 hours.

Table 2. The atomic force ratios for surface roughness and root mean square of the prepared films.

No.	Composite	Roughness average (nm)	Root mean square of roughness (nm)
1	PVC+nanocomp. (Before irradiation)	8.83	6.22
2	PVC+nanocomp. (after irradiation)	8.43	10.4
3	PS +nanocomp. (Before irradiation)	5.01	6.49
4	PS+nanocomp. . (after irradiation)	8.67	10.9

change was simple, which means that the additives preserved the polymer chips from changes and is evidence of their efficiency as optical stabilizers [38].

Measuring the rate of photodegradation of polymer films using an 8300 Shimadzu Fourier transform infrared FT-IR spectrophotometer within the range of 4000–400 cm^{-1}. The carbonyl (I_{CO}) and hydroxyl (I_{OH}) indices were determined by comparing the FT-IR absorption peak at 1726 and 3412 cm^{-1} reference PS, PVC with the remaining peaks and by monitoring the changes in the carbonyl and hydroxyl peaks [39, 40] as shown in (Fig. 7), the band index method is a designation of the method in question, utilizing equation (8,9); also, through (Fig. 8), the additives showed optical stability for PS and PVC through the three coefficients: polyene (I_{OP}), hydroxyl (I_{OH}) and carbonyl (I_{CO}). The sequence of nano in its optical inhibitory effect on PVC was as follows:

PVC < PS < PVC+ nanocomp. < PS + nanocomp.

The effectiveness of the polymeric membranes with the presence of cobalt nanocompact (PS+ nanocomp.) was better than (PVC+ nanocomp.), and both were better than pure PS and PVC polymers, as all coefficients decreased upon addition of the nanocomplex, especially at irradiation time of 300 hours. (I_{CO}) decreased by 0.754 and 0.482, and (I_{PO}) decreased by 0.233 and 0.325 when compared to (PVC and PS) alone, and (I_{OH}) decreased by 0.422 only for PVC because PS does not contain hydroxyl groups that were exposed to the same Radiation conditions due to the increased surface area and thus increased ability to bind to free radicals and the ability to stabilize electronically, due to the large number of connections allowing the electronic charge to distribute and then dissipate outside the surface of the polymer after the disappearance of the effect (sunlight). Thus, it is not affected by environmental conditions such as light and heat, and this makes the addition ideal for increasing the stability of the polymer for a long time, it is clear that the addition is ideal for the stability of the polymer for a long period as the nano-additives protect the polymer films during exposure to ultraviolet radiation, absorption, or screening, peroxide analysis, and radical scavenger mechanisms.

The fragmentation rate of polymer films was measured using UV spectroscopy

The results of irradiation of PS and PVC with

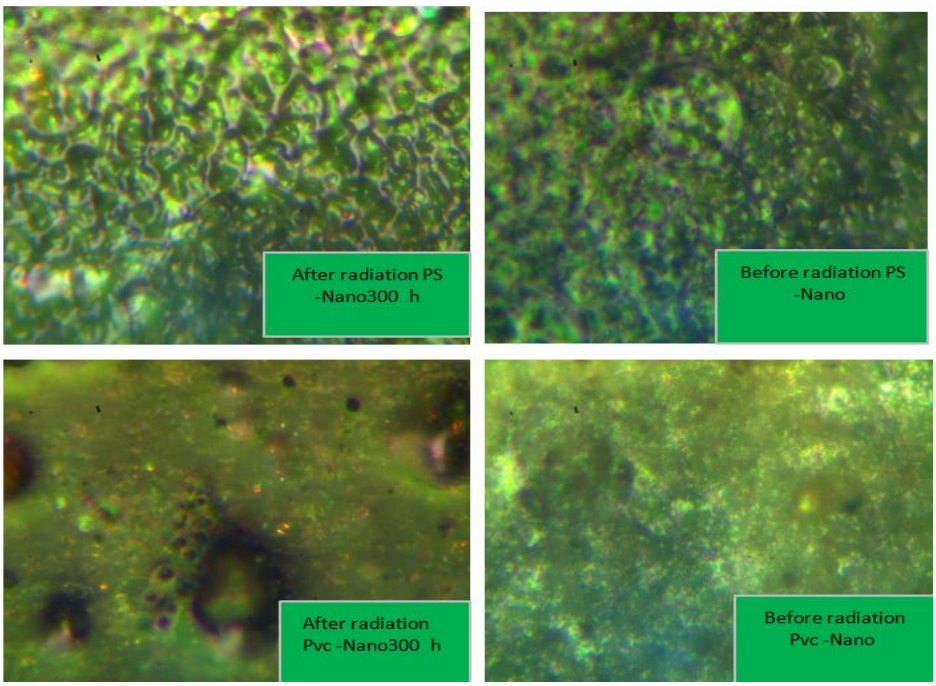

Fig. 6. The microscopic imaging of the polymers without and with the addition of the cobalt nanocomplex.

and without the nano complex (40µm thick) are shown in Fig. 9, which showed low values of the photodecomposition rate constant (kd), which is subject to the first order as shown in Eq. 5.

$$\ln \ln (A_t - A_\infty) = \ln \ln (A_\circ - A_\infty) - kdt \qquad (5)$$

where: = A_o represents the absorbance of the polymer film containing the additive before irradiation, A_t = represents the absorbance of the polymer film after irradiation time, and A_∞ = represents the absorbance of infinity [41]. Table 3 shows the values of the photodissociation rate constants kd of the nano complex with PS and PVC

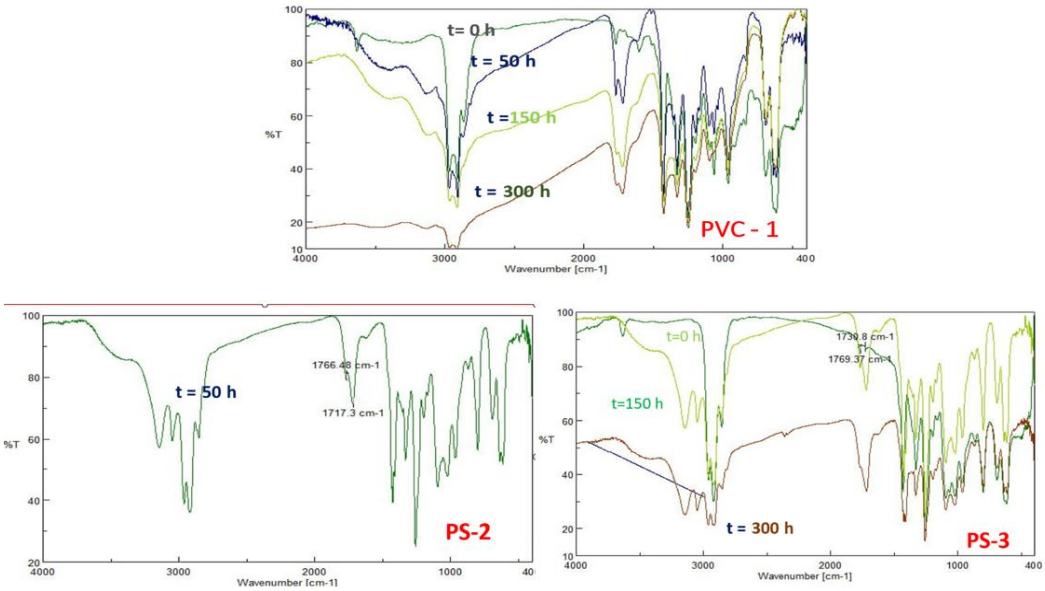

Fig. 7. (a) The FT-IR spectra, (PVC-1) at time (0, 50,150,300) hours, (PS-2) at (50) hours, and (PS-3) at (0,150,300) hours polymer films with the nanocomplex before and after irradiation.

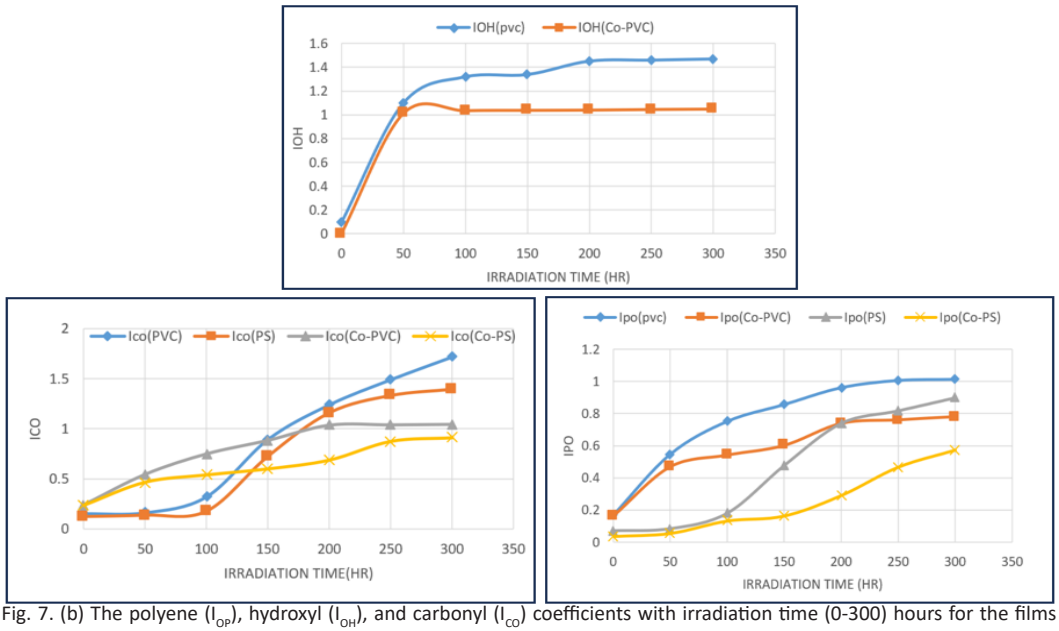

Fig. 7. (b) The polyene (I_{OP}), hydroxyl (I_{OH}), and carbonyl (I_{CO}) coefficients with irradiation time (0-300) hours for the films calculated through FT-IR.

films at 365 nm wavelength.

This means that the nano complex acted as a photostabilizer to inhibit the photooxidation process of the polymer and make it stable against UV rays. This is consistent with the infrared measurements of the coefficient values (I_{OP}, I_{CO}, I_{OH}).

PVC > PS > PVC+ nanocomp. > PS + nanocomp

Determination of the viscosity of the average molecular weight using the viscometer method

To calculate the average molecular weight, the "Mark-Houwink equation" shown below was used Eq. 6,

$$\eta = K \underline{Mv}^{\alpha} \quad (6)$$

Where α and K are constants that rely on the polymer solvents related to temperature, [η] is intrinsic viscosity.

The intrinsic viscosity of a polymer solution was measured using an "Ostwald U-tube" viscometer. The solutions were made by dissolving the polymer in benzene as a solvent (g/100 ml) at a specific viscosity of 25 °C [spη] was used to calculate the Eq. 7

$$[\eta sp] = \eta re - 1 \ , \qquad \eta re = t/t_o \quad (7)$$

Where: [ηsp] = specific viscosity, ηre = relative viscosity, t = the flow time of the polymer solution, t_0 = the flow time of the pure solvent.

To convert to intrinsic viscosity, the following equation was used Eq. 8:

$$[\eta] = (\sqrt{\frac{2}{C}})(\eta sp - \ln \eta re)^{1/2} \quad (8)$$

Where: C= the concentricity of solution polymers (g/100 ml)

The average molecular weight of (PVC) and (PS) films was calculated from the intrinsic viscosity equation (6) dissolved in tetrahydrofuran (THF) solution.

$$[\eta] = 11.8 \times 10^{-4} \ \underline{M_v}^{0.73} \quad (9)$$

The changes of Mu with irradiation time for PVC and PS films during the presence of the nano

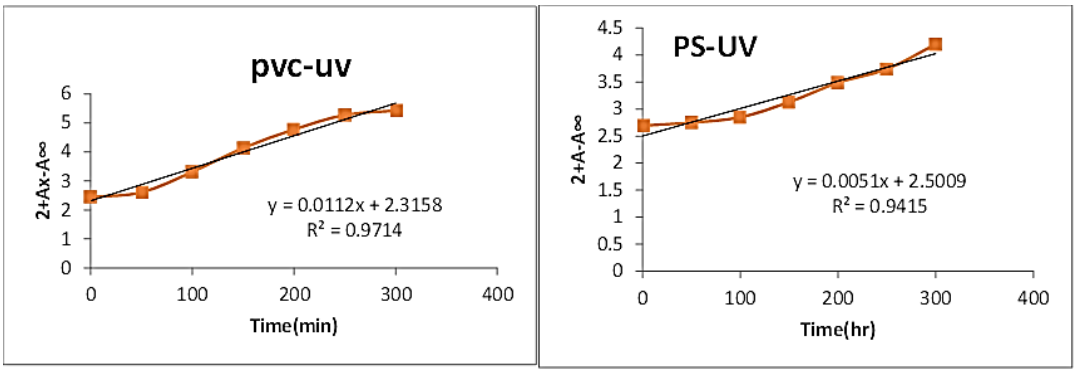

Fig. 8. The change of ln (At-A∞) with irradiation time for PVC and PS films.

Table 3. Values of the photodissociation rate constants of the nanocomplex were added to PS and PVC films at a wavelength of 365 nm.

samples	$k_d(h^{-1})$
PVC	$112*10^{-4}$
PVC+ nanocomp.	$24*10^{-4}$
PS	$71*10^{-4}$
PS+ nanocomp.	$21*10^{-4}$

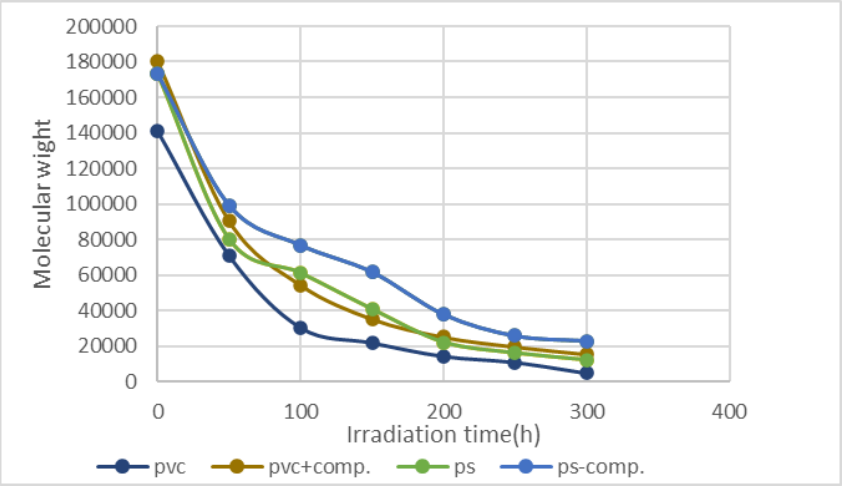

Fig. 9. The change of M_u with the irradiation time of the films.

Table 4. The change of M_u with irradiation time for PVC and PS films in the presence of the nano complex.

Sample	Time h						
	0	50	100	150	200	250	300
PVC	140852	70916	30463	21983	14398	10981	4931
PVC+ nanocomp.	180225	90371	54426	35313	25125	19657	15419
PS	173246	80193	61214	40887	22184	16126	12204
PS+ nanocomp.	173246	99331	76854	61781	37870	25761	22876

complex can be found in Table 4.

The decomposition of the films in Fig. 10 was followed without and with the addition of the viscosity ratio calculation of the molecular weight, where the results showed a decrease in the molecular weight of PVC and PS compared to the presence of the complex.

CONCLUSION

The new nanocomplex synthesis method easily without side effects and with very high efficiency in ultrasound waves is better than the methods of preparing nanocomplexes or additives used in previous research or non-nanocomplexes. The new nano complex can be used in many industrial applications as additives because the material is characterized by a lower energy gap compared to any micro complex and is considered a successful way to preserve the life of the polymer from breakage resulting from the effect of sunlight. Nanocomplex is an excellent alternative to the additives used to date, which are characterized by their small size because nanocomplex integrates with the organic chains in an excellent way and is distributed within the polymer and gives good results compared to nano metal oxides which aggregate or require the addition of another material to help distribute them within the polymer. The results showed that the prepared films are not affected by environmental conditions such as light and temperature and confirmed the relatively high melting points according to the low rate of loss of molecular weight Mv and the percentage of weight loss of the polymer films. The rate of measuring the hydroxyl (I_{OH}) and carbonyl (I_{CO}) coefficients also supports this conclusion. The carbonyl, hydroxyl, and polyene coefficients of the polymeric membranes grafted with cobalt nano compact were lower than the pure polymeric membranes, indicating that they

act as optical stabilizers. The optical inhibition effectiveness of polyvinyl and polystyrene can be arranged as follows:

PVC < PS < (PVC+ nanocomp.) < (PS + nanocomp.)

ACKNOWLEDGEMENTS

The authors thank the Chemistry Department, College of Science, University of Wasit, Iraq, for this work's logistic support.

CONFLICT OF INTEREST

The authors declare that there is no conflict of interests regarding the publication of this manuscript.

REFERENCES

1. Zafar W, Sumrra SH, Chohan ZH. A review: Pharmacological aspects of metal based 1,2,4-triazole derived Schiff bases. Eur J Med Chem. 2021;222:113602.
2. Sharma BP, Adhikari Subin J, Marasini BP, Adhikari R, Pandey SK, Sharma ML. Triazole based Schiff bases and their oxovanadium(IV) complexes: Synthesis, characterization, antibacterial assay, and computational assessments. Heliyon. 2023;9(4):e15239.
3. Ali AA, Al-Jorani KR, Merza MM. Synthesis and Characterization of New Schiff Base Containing 1,2,4-Triazole-3-thione Moiety and Its Complexes with Some Transition Metal Ions: Spectroscopic and Computational Studies. Russ J Gen Chem. 2024;94(2):471-487.
4. Ali A, Al-Hassani R, Hussain D, Jabir M, Meteab H. Anti-Proliferative Activity and Tubulin Targeting of Novel Micro and Nanoparticles Complexes of 4-Amino-3-Thion-1,2,4-Triazole Derivatives. Nano Biomed Eng. 2020;12(1).
5. Lombardi L, Bandini M. Graphene Oxide as a Mediator in Organic Synthesis: a Mechanistic Focus. Angew Chem Int Ed. 2020;59(47):20767-20778.
6. Al-Jorani KR, Abbood AF, Ali AA, Kadhim MM, Hamdan SD. Synthesis, characterizations, and computational studies of new tetrasubstituted imidazole containing a benzothiazole moiety. Struct Chem. 2022;34(3):1143-1156.
7. Yazdani M, Edraki N, Badri R, Khoshneviszadeh M, Iraji A, Firuzi O. Multi-target inhibitors against Alzheimer disease derived from 3-hydrazinyl 1,2,4-triazine scaffold containing pendant phenoxy methyl-1,2,3-triazole: Design, synthesis and biological evaluation. Bioorg Chem. 2019;84:363-371.
8. Zafar W, Ashfaq M, Sumrra SH. A review on the antimicrobial assessment of triazole-azomethine functionalized frameworks incorporating transition metals. J Mol Struct. 2023;1288:135744.
9. Thaer Ali Albayati M, Khudhair Hussein M. The Relationship between Toxic Leadership and Emotional Abuse: An Applied Study in the Iraqi Hotel Sector. Iraqi Journal for Administrative Sciences. 2025;21(84):56-70.
10. Yousif E, Haddad R. Photodegradation and photostabilization of polymers, especially polystyrene: review. SpringerPlus. 2013;2(1).
11. Ali AA, Al-Jorani KR, Abbood AF. Synthesis, Characterization, and Implementations for Dye Solar Cell of New Hematite Nanoparticles Using Tetrasubstituted Imidazole Containing a Benzimidazole Moiety. Russ J Gen Chem. 2023;93(7):1783-1790.
12. Zhang M, Biesold GM, Choi W, Yu J, Deng Y, Silvestre C, et al. Recent advances in polymers and polymer composites for food packaging. Mater Today. 2022;53:134-161.
13. Neme K, Nafady A, Uddin S, Tola YB. Application of nanotechnology in agriculture, postharvest loss reduction and food processing: food security implication and challenges. Heliyon. 2021;7(12):e08539.
14. Ali G, El-Hiti G, Tomi I, Haddad R, Al-Qaisi A, Yousif E. Photostability and Performance of Polystyrene Films Containing 1,2,4-Triazole-3-thiol Ring System Schiff Bases. Molecules. 2016;21(12):1699.
15. Al-khazraji SM. Antidiarrhoeal activity of Peucedanum pastinacifolium in Rodents. Research Journal of Pharmacy and Technology. 2018;11(10):4667.
16. Balakit AA, Ahmed A, El-Hiti GA, Smith K, Yousif E. Synthesis of New Thiophene Derivatives and Their Use as Photostabilizers for Rigid Poly(vinyl chloride). International Journal of Polymer Science. 2015;2015:1-10.
17. Kaleab Tesfaye T, Eleni Tesfaye T, Mekibib Kassa T, Geleta A, Berhanu B, Kebebush G, et al. Spatial distribution of COVID-19 in Ethiopia - geospatial analysis. Global Journal of Infectious Diseases and Clinical Research. 2022;8(1):001-007.
18. Yousif E, Ahmed DS, Ahmed AA, Hameed AS, Muhamed SH, Yusop RM, et al. The effect of high UV radiation exposure environment on the novel PVC polymers. Environmental Science and Pollution Research. 2019;26(10):9945-9954.
19. Salam B, El-Hiti GA, Bufaroosha M, Ahmed DS, Ahmed A, Alotaibi MH, et al. Tin Complexes Containing an Atenolol Moiety as Photostabilizers for Poly(Vinyl Chloride). Polymers. 2020;12(12):2923.
20. Majeed A, Yousif E, El-Hiti GA, Ahmed DS, Ahmed AA. Stabilization of Poly(Vinyl Chloride) Containing Captopril Tin Complexes against Degradation upon Exposure to Ultraviolet Light. Journal of Vinyl and Additive Technology. 2020;26(4):601-612.
21. Jubier NJ, Al-Jorani KR, Ali AA, Al –Bayaty SA, Al-Uqaily RAH. Thermal degradation assessment, impact strength, and hardness of combination epoxy and polystyrene powder composite. Kuwait Journal of Science. 2024;51(4):100271.
22. Kadhium SS, Hussen EM, Mageed ZN, Abed AH, Mohammed HH. Study the Photo-degradation of poly styrene –co-butadiene in presence of Ni complex and TiO_2. IOP Conference Series: Materials Science and Engineering. 2020;871(1):012026.
23. Maafa I. Pyrolysis of Polystyrene Waste: A Review. Polymers. 2021;13(2):225.
24. Zhang Y, Sun T, Zhang D, Shi Z, Zhang X, Li C, et al. Enhanced photodegradability of PVC plastics film by codoping nano-graphite and TiO_2. Polymer Degradation and Stability. 2020;181:109332.
25. Martín AJ, Mondelli C, Jaydev SD, Pérez-Ramírez J. Catalytic processing of plastic waste on the rise. Chem. 2021;7(6):1487-1533.
26. Jasim BE, Ahmed AA, Aboud NAA. A Comparative Study of the Photostabilization of Polyvinyl Chloride with Nano and Micro Nickel Oxide. Baghdad Science Journal. 2023.
27. Jasim BE, Aboud NAA, Rheima AM. Nickel oxide nanofibers manufactured via sol-gel method: synthesis, characterization and use it as a photo-anode in the dye sensitized solar cell. Digest Journal of Nanomaterials and Biostructures. 2022;17(1):59-64.